JOURNAL OF MAGNETIC RESONANCE **130,** 51–57 (1998)
ARTICLE NO. MN971273

Optimization of Signal Intensity and T_1-Dependent Contrast with Nonstandard Flip Angles in Spin-Echo and Inversion-Recovery MR Imaging

Jean-Marie Bonny, Loic Foucat, Wilfried Laurent, and Jean-Pierre Renou

SRV unité STIM, INRA-Theix, 63122 Saint-Genès-Champanelle, France

Received March 11, 1997; revised September 10, 1997

Theoretical expressions of flip angle values maximizing signal intensity and T_1-dependent contrast are derived for spin-echo and inversion-recovery sequences. Experimental data and theoretical predictions are closely correlated for experiments carried out on phantoms, despite the nonideal shape of the RF refocusing pulse used for slice selection. The use of nonstandard angles is justified when rapid MR acquisitions are needed and/or large T_1 species must be imaged with refocused sequences.

INTRODUCTION

In conventional spin-echo (SE) imaging, a $\pi/2$ nutating pulse is used followed by one or several π refocusing pulses. As pointed out by several authors (*1–4*), by selecting a nutating pulse angle larger than $\pi/2$, steady-state conditions should result in increased signal intensity and thus a higher signal-to-noise ratio. However, it has been shown for spoiled partial saturation sequences in steady state that T_1-dependent contrast and signal intensity are not maximal for the same flip angle (*5, 6*). Moreover, it has been demonstrated numerically that varying the inversion or excitation pulse tip angles can induce a significant enhancement in signal intensity and contrast also in inversion-recovery (IR) imaging (*7, 8*).

This work examines the mathematical processes leading to the expression of pulse angle values which maximize signal intensity for SE and IR sequences in steady state, and can compensate for various field inhomogeneities (background field inhomogeneities, local susceptibility and chemical shift effects). Along the same lines, we propose algebraic guidelines for deriving pulse angle values, which maximize T_1-dependent contrast. By this means, we wished to optimize MR conditions when the repetition time (TR) to T_1 ratio is low, i.e., when rapid MR acquisitions are needed and/or large T_1 species must be imaged.

THEORY

Expression of SE Signal Intensity

The general form of a SE sequence with a single refocusing pulse is given by

$$[\alpha_x\text{–TE/2–}\beta_y\text{–TE/2–echo–(TR–TE)–}], \qquad [1]$$

where α and β are respectively the nutating and refocusing pulse angles about the axis denoted by the subscript. Here, we consider no coherence of transverse magnetization between cycles of excitation (because of T_2 relaxation when TR $\gg T_2$ or by appropriate spoiling) and we neglect the effect of spin–lattice relaxation during the TE delay (i.e., TE $\ll T_1$). Moreover, we assume complete dephasing of the transverse magnetization at TE/2. On these assumptions, the intensity of the observed SE signal, rising at the echo time TE, is proportional to the transverse magnetization M_T equal to (*9*)

$$M_T = f_I(\alpha, \beta; E_1)\cdot M_0(1 - E_1)E_2. \qquad [2]$$

The following function f_I expresses the steady-state effect of the longitudinal z magnetization

$$f_I(\alpha, \beta; E_1) = \frac{1}{2}\frac{\sin\alpha(1 - \cos\beta)}{1 - E_1\cos\alpha\cos\beta}, \qquad [3]$$

and E_1 and E_2 are the contributions of relaxation expressed by

$$E_1 = \exp\left(-\frac{\text{TR}}{T_1}\right) \qquad E_2 = \exp\left(-\frac{\text{TE}}{T_2}\right). \qquad [4]$$

Maximization of SE Signal Intensity Using Nonstandard Flip Angles

For given values of T_1 and TR, signal intensity is maximum for a particular pair of angle values (α_I, β_I) that maximize f_I (see Eq. [3]). These parameters can be obtained by setting simultaneously $\partial f_I/\partial\alpha$ and $\partial f_I/\partial\beta$ equal to zero (necessary stationary conditions), whence f_I is maximized for β_I equal to π (for any E_1) while α_I depends on E_1 (see Fig. 1) as (*1, 3*)

1090-7807/98 $25.00

$$\alpha_I = \arccos(-E_1) = \pi - \alpha_E, \quad [5]$$

where α_E is the Ernst angle (*10*). As steady-state function f_I is equal to 1 for the standard values $\alpha = \pi/2$ and $\beta = \pi$, the expression $f_I(\alpha_I, \beta_I; E_1)$ gives the maximum theoretical enhancement of signal intensity that can be reached using the large optimal nutating pulse angle α_I ($=\pi - \alpha_E$) in comparison with the common SE sequence

$$f_I(\alpha_I, \beta_I; E_1) = (1 - E_1^2)^{-1/2}. \quad [6]$$

This quantity is depicted in Fig. 2.

Maximization of T_1-Dependent Contrast Using Nonstandard Flip Angles

T_1-dependent contrast is related to the signal intensity differences between tissue types induced by differing T_1 values (*11*). Hence for a slight difference in ΔT_1, T_1 contrast takes a differential form proportional to the derivative of M_T (see Eq. [2]) with respect to T_1 (*6*), i.e.,

$$\Delta M_T \approx \frac{\partial M_T}{\partial T_1} \Delta T_1, \quad [7]$$

where

$$\frac{\partial M_T}{\partial T_1} = f_C(\alpha, \beta; E_1)\dot{E}_1 M_0 E_2$$

$$\dot{E}_1 = \frac{\partial E_1}{\partial T_1} = \frac{TR}{T_1^2} E_1 \quad [8]$$

and

$$f_C(\alpha, \beta; E_1) = -\frac{1}{2}\frac{\sin\alpha(1 - \cos\beta)(1 - \cos\alpha\cos\beta)}{(1 - E_1\cos\alpha\cos\beta)^2}. \quad [9]$$

This expression means that as for a spoiled partial saturation sequence (*6, 12, 13*), T_1 contrast accessible with an SE sequence under steady state depends not only on TR but also on α and β angle values. As previously discussed for signal intensity, T_1 contrast is thereby maximum for particular angle values α_C and β_C that maximize f_C, i.e., β_C equal to π (for any E_1) and α_C obtained by solving the equation

$$a_2\cos^2\alpha + a_1\cos\alpha + a_0 = 0 \quad [10]$$

with respectively

$$a_2 = 2 - E_1 \qquad a_1 = 1 + E_1 \qquad a_0 = 2E_1 - 1. \quad [11]$$

The root of Eq. [10] is given by (see Fig. 1)

$$\alpha_C = \pi - \arccos\left(\frac{2E_1 - 1}{2 - E_1}\right). \quad [12]$$

Given $|f_C(\pi/2, \pi; E_1)| = 1$, the maximum theoretical enhancement of T_1 contrast, obtained with the optimal nutating pulse angle α_C instead of $\pi/2$, is equal to

$$f_C(\alpha_C, \beta_C; E_1) = \frac{3\sqrt{3}}{4}(1 - E_1)^{-1/2}(1 + E_1)^{-3/2}. \quad [13]$$

This quantity is depicted in Fig. 2.

Expression of IR Signal Intensity

The standard IR sequence is simply a general SE preceded by an inversion pulse, i.e.,

$$[\pi\text{–TI–}\alpha_x\text{–TE/2–}\beta_y\text{–TE/2–echo–(TR–TE–TI)–}], \quad [14]$$

where TI is the inversion delay between the inversion and excitation pulses. The inversion pulse may also be followed by a gradient-recalled echo sequence. As indicated in the Introduction, this work deals exclusively with an inversion followed by a spin-echo formation. The inversion pattern enables us to null the signal intensity of a specific tissue and then enhance signals from other regions (if T_1 is different). Fluid-attenuated IR (FLAIR) and short TI IR (STIR) sequences are based on this principle to reduce or null the signal from fluid and fat (*14, 15*).

On the same assumptions as those made for the SE sequence, the intensity of the observed IR signal (at TI + TE) is proportional to (*7*)

$$M_T = g_I(\alpha, \beta; E_1) \cdot M_0(1 - 2E_1' + E_1)E_2. \quad [15]$$

The steady-state effect of the longitudinal *z* magnetization is given by

$$g_I(\alpha, \beta; E_1) = \frac{1}{2}\frac{\sin\alpha(1 - \cos\beta)}{1 + E_1\cos\alpha\cos\beta}, \quad [16]$$

where E_1' is the contribution of T_1 relaxation during TI, i.e.,

$$E_1' = \exp\left(-\frac{TI}{T_1}\right). \quad [17]$$

To null the magnetization of a tissue with a known spin–lattice relaxation time T_1^N, the following condition (see Eq. [15]) needs to be met,

$$1 - 2E'_1 + E_1 = 0, \quad [18]$$

leading us to choose an inversion delay equal to

$$\mathrm{TI} = T_1^{\mathrm{N}} \ln 2 - T_1^{\mathrm{N}} \ln\left[1 + \exp\left(-\frac{\mathrm{TR}}{T_1^{\mathrm{N}}}\right)\right]. \quad [19]$$

Maximization of IR Signal Intensity Using Nonstandard Flip Angles

Given that

$$g_{\mathrm{I}}(\pi - \alpha, \beta; E_1) = f_{\mathrm{I}}(\alpha, \beta; E_1), \quad [20]$$

and that f_{I} is maximized for $\alpha_{\mathrm{I}} = \pi - \alpha_{\mathrm{E}}$ and $\beta_{\mathrm{I}} = \pi$, we can derive that g_{I} is maximized for a refocusing angle β'_{I} equal to π (for any E_1) and a nutating angle α'_{I} equal to the Ernst angle (see Fig. 3) as

$$\alpha'_{\mathrm{I}} = \pi - \alpha_{\mathrm{I}} = \pi - (\pi - \alpha_{\mathrm{E}}) = \alpha_{\mathrm{E}}. \quad [21]$$

Also, the maximum signal intensity enhancement is the same for IR as for SE (see Eq. [6]) and is depicted in Fig. 2.

Maximization of T_1-Dependent Contrast Using Nonstandard Flip Angles

Applying Eq. [7] to Eq. [15], differential T_1 contrast for an IR sequence is given by

$$\frac{\partial M_{\mathrm{T}}}{\partial T_1} = g_{\mathrm{C}}(\alpha, \beta; E_1, E'_1) \cdot M_0 E_2 \quad [22]$$

with

$$g_{\mathrm{C}}(\alpha, \beta; E_1, E'_1) = \frac{1}{2}\frac{\sin\alpha(1 - \cos\beta)}{1 + E_1 \cos\alpha \cos\beta}(-2\dot{E}'_1 + \dot{E}_1) + \frac{1}{2}\frac{\sin\alpha\cos\alpha\cos\beta(1 - \cos\beta)}{(1 + E_1\cos\alpha\cos\beta)^2} \times (1 - 2E'_1 + E_1)\dot{E}_1 \quad [23]$$

and

$$\dot{E}'_1 = \frac{\partial E'_1}{\partial T_1} = \frac{\mathrm{TI}}{T_1^2} E'_1. \quad [24]$$

T_1 contrast is maximum for particular angle values α'_{C} and β'_{C} that maximize g_{C}, i.e., β'_{C} equal to π (for any E_1 and E'_1) and α'_{C} obtained by solving Eq. [10] with the following coefficients (see Fig. 3):

TABLE 1
T_1[a] and T_2[b] Values of Phantom Tubes

Tube	T_1 (ms)	T_2 (ms)
A	2436	567
B	2728	598
C	281.7	10.8
D	297.3	11.9
E	121.6	4.5
F	119.4	4.4

Note. Values were obtained by spectroscopy with IR[a] and CPMG[b] sequences.

$$a_0 = (-1 - 2E_1 + 2E'_1)\dot{E}_1 + 2E_1\dot{E}'_1$$
$$a_1 = (1 - E_1 + 2E_1E'_1)\dot{E}_1 - 2(1 + E_1^2)\dot{E}'_1$$
$$a_2 = (2 + E_1 - 4E'_1)\dot{E}_1 + 2E_1\dot{E}'_1. \quad [25]$$

EXPERIMENTAL

Instrumentation

All the experiments were performed on a Bruker AMX-400 NMR spectrometer, using a 9.4-T superconducting magnet with an 89-mm-diameter vertical bore, operating at 400 MHz for ^{1}H. The spectrometer was equipped with a micro-imaging accessory with 50-mm gradient coils. A Helmholtz coil with a 20-mm diameter is used for both radiofrequency (RF) transmission and signal reception.

Phantom Studies

Theoretical predictions were verified by performing phantom studies at variable flip angle values. Signal intensities, and thus contrasts, were measured on images of a phantom composed of six tubes of 5-mm diameter containing water doped with $MnCl_2$. The concentrations were chosen to simulate three pairs of tissues (tubes A–B, C–D, and E–F) with a slight difference in T_1 values. Table 1 gives T_1 and T_2 values for each tube that were separately determined by NMR spectroscopy at 25°C.

After magnitude reconstruction, the mean and standard deviation of signal intensities were measured inside a circular region of interest 5 pixels in diameter, which was manually centered in each tube.

MR Sequences

SE and IR sequences used a slice-selective π refocusing pulse with a three-lobe cardinal sine waveform (2-ms duration). The variable flip angle was obtained by adjusting the duration of a nonselective rectangular pulse. For the IR sequence, the whole magnetization was inverted using a nonselective π rectangular pulse (74-μs duration). Sequence

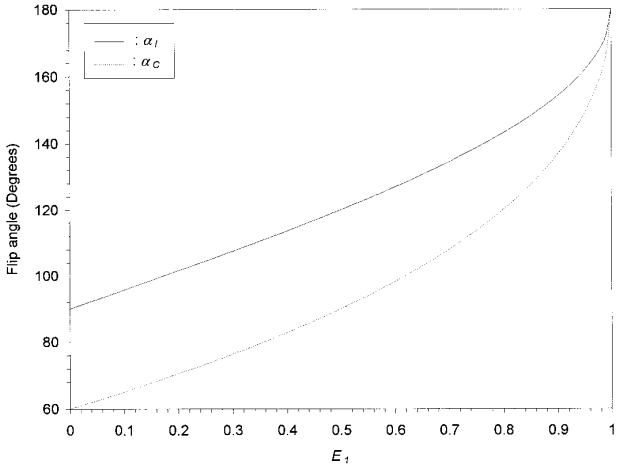

FIG. 1. Theoretical values of nutating angle maximizing signal intensity (solid line) and T_1 contrast (dashed line) for the SE sequence as a function of E_1.

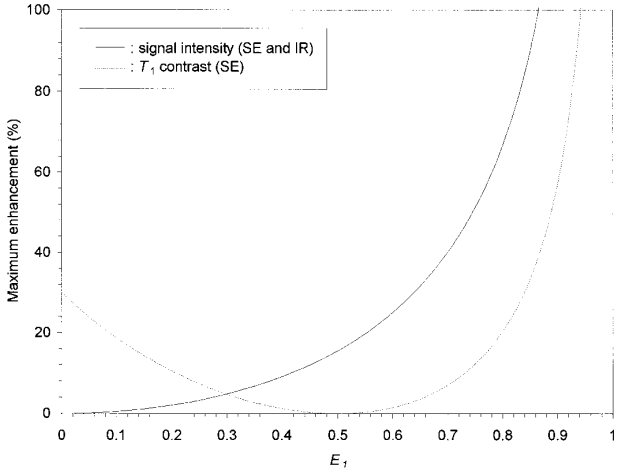

FIG. 2. Theoretical maximum enhancement of signal intensity (solid line) for the SE and IR sequences and T_1 contrast (dashed line) for the SE sequence as a function of E_1.

parameters were TR = 200 ms, TE = 4.38 ms, slice thickness 10 mm, field of view 18 mm, image matrix 256 × 256, eight averages, and an imaging bandwidth of 100 kHz. The inversion time TI of the IR sequence has been chosen to null the signal intensity tube D according to Eq. [19], i.e., TI = 83.5 ms. A spoiler gradient is applied after echo sampling to eliminate any coherence of transverse magnetization.

RESULTS

Theoretical Results

Suppose that a $(\pi - \alpha)$ nutating pulse and a π refocusing pulse are applied successively and that the effect of T_1 relaxation is neglected between these two pulses (i.e., for TE/2). There occurs a partial saturation where the net magnetization has nutated by an angle α from the z axis in the (yz) rotating plane (exactly, α for $[\pi - \alpha]_x - \pi_y$ and $-\alpha$ for $[\pi - \alpha]_x - \pi_x$). This is why the Ernst angle supplement (i.e., $\pi - \alpha_E$) and the Pelc–Buxton angle supplement (see Eq. [12]) maximize signal intensity and T_1 contrast, respectively. This explanation can be simply extended to the IR case by considering that the net magnetization is first inverted by a π pulse (see Eq. [21]).

Selecting the optimal nonstandard nutating angle for both SE and IR sequences, Fig. 2 shows that signal enhancement increases as E_1 increases (i.e., TR/T_1 decreases) as the steady-state effect is also enhanced.

For the SE sequence, Fig. 1 shows that α_I and α_C are significantly different (by about 20°). In practice, signal intensity and T_1 contrast maximization constraints are incompatible. Thus, two different acquisitions are required with larger tip angles as E_1 increases (i.e., as TR decreases).

In contrast, Fig. 3 shows for the IR sequence that α'_I and α'_C are close and decrease as E_1 increases. For a STIR sequence, a good compromise between signal intensity and T_1 contrast enhancement can therefore be reached by selecting a tip angle around the Ernst value (in particular when $E_1 = 0.5$, $\alpha'_I = \alpha'_C = \alpha_E$). However, if an accurate optimization of T_1 contrast is required, a second-order polynomial with coefficients given by Eq. [25] must be solved to determine the flip angle value α'_C. For E_1 below 0.8, there is only one meaningful root (with a module below one). For E_1 above 0.8, Eq. [25] yields two solutions (which are both represented in Fig. 3) and the value that affords the best T_1 contrast enhancement must obviously be chosen.

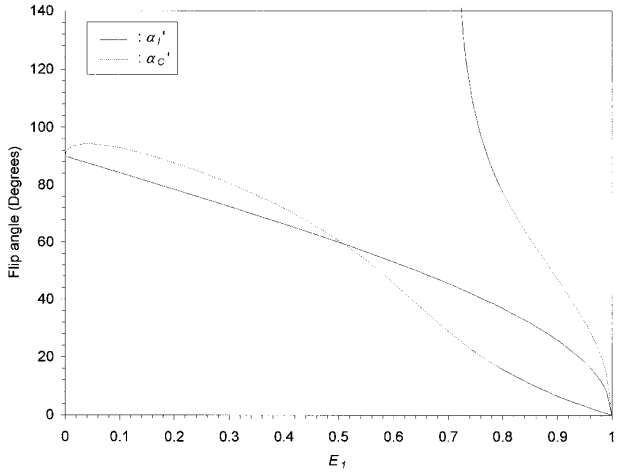

FIG. 3. Theoretical values of nutating angle maximizing signal intensity (solid line) and T_1 contrast (dashed line) for the IR sequence as a function of E_1 (variable T_1). α'_C is obtained for sequence parameters nulling the signal intensity of tube D according to Eq. [19]; i.e., TI = 83.5 ms for TR = 200 ms.

Magnitude reconstruction of images rectifies all negative values of signal intensity, to produce only positive values. Hence if signal polarity is not restored (*16*), the measured IR signal intensity is equal to the absolute value of expression [15]. While the considered T_1 contrast takes a differential form (slight difference in T_1), magnitude reconstruction has no influence on the theoretical expression of α'_C. Theory fails only when the considered contrast is between two materials with widely different longitudinal relaxation times T_1^a and T_1^b (a discrete problem according to Ref. *6*) and/or when $T_1^a < T_1^N < T_1^b$.

For SE sequence maximizing T_1 weighting (i.e., TR = T_1), signal intensity improvement using $\alpha_I = 112°$ is about 7.5%, whereas $\alpha_C = 81°$ affords a low contrast enhancement ($\approx$2%). Thus, nonstandard angles are especially justified for improving the signal intensity of T_1-weighted SE images (*17*). More generally, they enable us to enhance signal intensity or T_1 contrast of SE and IR images when rapid MR acquisitions are needed and/or large T_1 species must be imaged.

Shortening TR while increasing the number of acquisitions may have some beneficial effects (*18, 19*). Indeed, by using this approach combined with the nonstandard flip angles α_I and α_C, it is possible to improve signal-to-noise and T_1 contrast-to-noise ratios (respectively S/N and C/N) of a T_1-weighted SE image (with TR = T_1 and $\alpha = \pi/2$), while keeping the acquisition time constant. For the SE sequence the loss of S/N and C/N due to a TR shortening is more than compensated for by an increase in the number of averages with the same factor N. With N = 2, 4, and 8, S/N and C/N increase respectively by 3, 4, and 11% and 16, 21, and 22%. However, the same calculations applied to the IR sequence do not show any improvement either for S/N or for C/N.

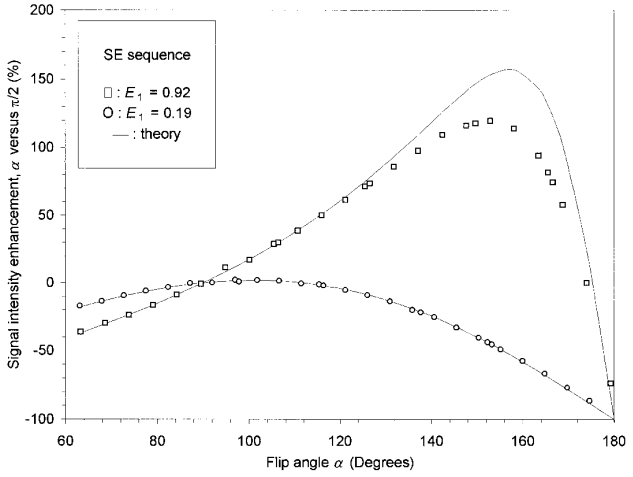

FIG. 4. Comparison of experimental and theoretical evolution of the SE signal intensity as a function of nutating angle value α.

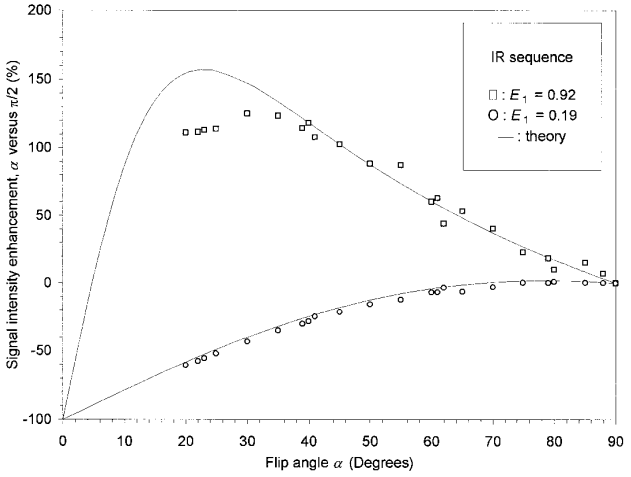

FIG. 5. Comparison of experimental and theoretical evolution of the IR signal intensity as a function of nutating angle value α.

Phantom Studies

Figure 4 for the SE sequence and Fig. 5 for IR show a close similarity between experimental and theoretical signal intensity enhancement as a function of the tip angle value α. The deviation between these two curves around the maximum can be explained by the effect of the nonideal slice profile of the refocusing soft pulse. This means integrating steady-state signals characterized by complete refocusing in the center of the slice and incomplete refocusing in its outer wings. It is observed that these imperfections become more marked when steady-state conditions are preponderant, i.e., when the flip angle value markedly deviates from $\pi/2$ and/or for large values of E_1 (according to Ref. *13*).

Despite the slice profile imperfections, it must be noted that the experimental flip angle value that maximizes signal intensity is near the theoretical value for both sequences. Moreover, there is also a close similarity between experimental and theoretical T_1 contrast enhancement as a function of the tip angle value α in Figs. 6 and 7 (even though contrast measurements are more sensitive to noise).

DISCUSSION

The use of a large tip angle value as TR decreases in SE imaging results in an increase in RF energy deposition in the object being imaged and so in RF transmitter power requirements. To circumvent this drawback which can limit *in vivo* applications, RF pulses limiting specific absorption rates (especially soft pulses) should be used. Also, by selecting a nominal flip angle value maximizing signal intensity, SE or IR images become more sensitive to spatial variations of RF transmission field and especially to overflipping and underflipping of magnetization (respectively for SE and IR), since in this range a small

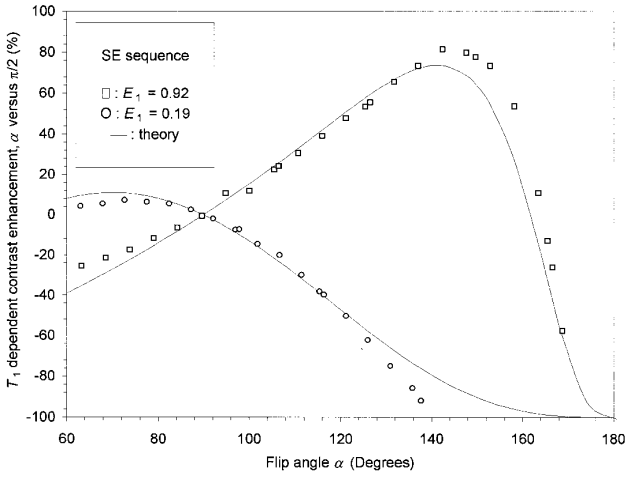

FIG. 6. Comparison of experimental and theoretical evolution of the SE T_1 contrast as a function of nutating angle value α.

variation in flip angle value produces a large deviation of signal intensity (see Fig. 4 and Fig. 5). Finally, RF pulse amplitudes must be calibrated to induce accurate flip angle values. Procedures have been described for this (*20*) that do not, however, prevent the angle values from varying through spatial inhomogeneities of the B_1 transmission field. An alternative approach would be to use amplitude- and phase-modulated adiabatic pulses that both generate arbitrary and uniform flip angles despite large B_1 inhomogeneities and limit specific absorption rate (*21*).

The above theoretical expressions of signal intensity (see Eqs. [2] and [15]) were derived from the Bloch equations neglecting the effect of spin–lattice relaxation during the TE delay. If this assumption is not fulfilled, the SE and IR amplitudes become proportional respectively to

$$M_T = f_I(\alpha, \beta; E_1) \cdot M_0(1 - hE_1)E_2, \quad [26]$$

$$M_T = g_I(\alpha, \beta; E_1) \cdot M_0(1 - 2E_1' + hE_1)E_2, \quad [27]$$

with

$$h = \cos\beta + \exp\left(\frac{TE}{2T_1}\right) \cdot (1 - \cos\beta). \quad [28]$$

When $\beta = \pi$ and TE is not short compared to T_1 the values α_I and α_I' of optimal excitation angles that maximize signal intensity are unchanged because the expressions of signal intensity have the same dependence on α in Eqs. [26] and [27] and in Eqs. [2] and [15]. Numerical computations have shown that the angle value α_C which maximizes T_1 contrast for the SE sequence is higher than the one derived in Eq. [12]. It increases steadily as TE tends to TR, but the angle supplement is never larger than 15° when TE $< T_1$.

For the IR sequence the inversion time is shifted compared to the value given by Eq. [19] and TI is now equal to

$$TI = T_1^N \ln 2 - T_1^N \ln\left[1 + h \cdot \exp\left(-\frac{TR}{T_1^N}\right)\right], \quad [29]$$

whereas, the angle value which maximizes T_1 contrast for the IR sequence is very close to α_C'. For both SE and IR cases, T_1 relaxation during TE induces a rapid decrease of T_1 contrast which can be attained with these sequences.

This paper addresses the case of a spin echo acquired after an odd (i.e., one) number of refocusing pulses. It should be distinguished from the case of an even number of refocusing pulses that corresponds to the fast optimal angle spin echo with a short TE (FATE) sequence (*4, 22*). For an even number of refocusing pulses the optimum excitation angle at which maximum signal intensity or T_1-dependent contrast occurs is equal to $(\pi - \alpha)$, where α is the optimum excitation angle calculated for an odd number of refocusing pulses (*23*).

Vinitski *et al.* have suggested that an arbitrary inversion angle can be used to partially invert the magnetization (*7*) and then to shorten the inversion delay TI. It affects the optimal values of α_I' and α_C' only if there is a residual transverse magnetization just before the excitation pulse. Thus, these theoretical expressions are not acceptable when the inversion pulse is significantly lower than π and/or when the TI to T_2 ratio is too small. Nevertheless, this drawback can possibly be circumvented by applying a spoiler gradient between the inversion and the excitation pulses.

CONCLUSION

The use of nonstandard angles theoretically described here is justified for enhancing signal intensity and T_1-dependent

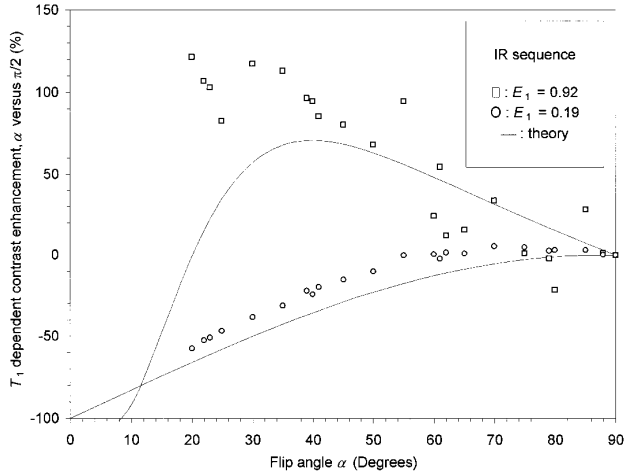

FIG. 7. Comparison of experimental and theoretical evolution of the IR T_1 contrast as a function of nutating angle value α.

contrast in steady-state SE and IR with a short TE. It enables us to optimize MR conditions for a short TR to T_1 ratio (below 5). Such sequences are especially designed for acquiring T_1-weighted images with (for IR) or without (for SE) signal attenuation of another species (for example, fat) and free of artifacts coming from various field inhomogeneities. Consequently, signal intensity or T_1 contrast of long T_1 substances can be significantly enhanced.

ACKNOWLEDGMENT

This work has been supported by the European Union (AIR Project CT96-1107).

REFERENCES

1. T. J. Provost and R. E. Hendrick, *Magn. Reson. Imaging* **4,** 105 (1986).
2. S. Vinitski, D. G. Mitchell, J. Szumowski, D. L. Burk, and M. D. Rifkin, *Magn. Reson. Imaging* **8,** 131 (1990).
3. A. D. Elster and T. J. Provost, *Invest. Radiol.* **28,** 944 (1993).
4. G. Diiorio, J. J. Brown, J. A. Borrello, W. H. Perman, and H. H. Shu, *Magn. Reson. Imaging* **13,** 39 (1995).
5. R. B. Buxton, R. R. Edelman, B. R. Rosen, and T. J. Brady, *Proc. SMRM* **3,** 661 (1986).
6. N. J. Pelc, *Magn. Reson. Med.* **29,** 695 (1993).
7. S. Vinitski, S. Albert, D. G. Mitchell, T. A. Tasciyan, and M. D. Rifkin, *Magn. Reson. Imaging* **10,** 207 (1992).
8. C. J. G. Bakker, T. D. Witkamp, and W. M. Janssen, *Magn. Reson. Imaging* **9,** 323 (1991).
9. F. Franconi, F. Seguin, C. B. Sonier, A. Le Pape, and S. Akoka, *Med. Phys.* **22,** 1763 (1995).
10. R. R. Ernst and W. A. Anderson, *Rev. Sci. Instrum.* **37,** 93 (1966).
11. F. W. Wehrli, J. R. MacFall, G. H. Glover, N. Grisby, V. Haughton, and J. Johanson, *Magn. Reson. Imaging* **2,** 3 (1984).
12. R. B. Buxton, R. R. Edelman, B. R. Rosen, G. L. Wismer, and T. J. Brady, *J. Comput. Assist. Tomogr.* **11,** 7 (1987).
13. W. Hänicke, K.-D. Merboldt, and J. Frahm, *J. Magn. Reson.* **77,** 64 (1988).
14. G. M. Bydder and I. R. Young, *J. Comput. Assist. Tomogr.* **9,** 659 (1985).
15. S. J. White, J. V. Hajnal, I. R. Young, and G. M. Bydder, *Magn. Reson. Med.* **28,** 153 (1992).
16. Q.-S. Xiang, *J. Magn. Reson. Imaging* **6,** 775 (1996).
17. D. H. Feiglin, W. Sattin, T. J. Provost, and E. M. Bellon, *J. Magn. Reson. Imaging* **1,** 235 (1991).
18. W. A. Edelstein, P. A. Bottomley, H. R. Hart, and L. S. Smith, *J. Comput. Assist. Tomogr.* **7,** 391 (1983).
19. R. E. Hendrick, F. D. Newman, and W. R. Hendee, *Radiology* **156,** 749 (1985).
20. B. Foerster, A. Tannús, and H. Panepucci, *J. Magn. Reson. A* **108,** 89 (1994).
21. S. Conolly, G. Glover, D. Nishimura, and A. Macovski, *Magn. Reson. Med.* **18,** 28 (1991).
22. T. C. Mills, D. A. Ortendahl, N. M. Hylton, L. E. Crooks, J. W. Carlson, and L. Kaufman, *Radiology* **162,** 531 (1987).
23. S. Vinitski and R. H. Griffey, Abstracts of the International Society of Magnetic Resonance in Medicine, 8th Annual Meeting, Amsterdam, p. 1162 (1989).